



Enabling Science through European Electron Microscopy

Report on improved calibration routines

Deliverable D4.4 – version 1

Estimated delivery date:	30 th June 2021
Actual delivery date:	23 rd of June 2021
Lead beneficiary:	UANTWERP
Person responsible:	Johan Verbeeck
Deliverable type:	<input checked="" type="checkbox"/> R <input type="checkbox"/> DEM <input type="checkbox"/> DEC <input type="checkbox"/> OTHER <input type="checkbox"/> ETHICS <input type="checkbox"/> ORDP
Dissemination level:	PUBLIC

Grant Agreement No:	823802
Funding Instrument:	Research and Innovation Actions (RIA)
Funded under:	H2020-INFRAIA-2018-1: Integrating Activities for Advanced Communities
Starting date:	01.01.2019
Duration:	48 months



Table of contents

Revision history log	3
Introduction.....	4
Image calibration.....	4
Image calibration with fringe patterns.....	4
Automated collection of reference holograms	4
Automated routines for eliminating centre-bands	5
New calibration procedure using multiple reference holograms	6
Diffraction calibration with a sample-space deflector	7
Improved corrector alignment	8
Future development.....	10
Software	11
References.....	11

Revision history log

Version number	Date of release	Author	Summary of changes
V0.1	19/01/2020	Johan Verbeeck	First draft of the deliverable
V1	21/06/2021	Peter van Aken	Approval of the deliverable

Introduction

While modern transmission electron microscopes provide a wealth of information from nanoscale samples with atomic spatial resolution, a microscope's accuracy is only as good as its calibrations. This calls for improved calibrations procedures, ideally automated, with an emphasis on straightforward portability between different microscopes to ensure reproducibility.

This deliverable D4.4 "Report on improved calibration routines" summarises recent developments associated with ESTEEM3 towards more accurate and reproducible measurements.

Image calibration

Calibration of TEM is commonly done by imaging and measuring (by hand) a known object at a variety of magnifications. This tedious and time-consuming procedure is typically only performed during microscope installation, and rarely repeated even after major repairs. This is vulnerable firstly to human error, and secondly to uncertainty over the reference sample (e.g. fabrication-induced strain) and thirdly to potential long-term drifts. Having calibration methods, which are widely reproducible and can be easily automated would help ensure the accuracy of the data obtained from the microscopes.

Image calibration with fringe patterns

Electron holograms contain valuable information concerning the atomic structure of crystalline samples, including mechanical strain, but also the local electrostatic and magnetic fields that permeate the material and the surrounding vacuum. This information is encoded in the phase of the hologram fringes. Unfortunately, the phase also contains unwanted contributions that arise from a number of other sources such as the imperfections of the biprism wire, geometrical distortions from the projector lenses of the microscope, and distortions from the detector used to acquire the hologram intensities. Artefacts are also caused by the phase reconstruction process itself, notably from cross-talk between the centre-band of the hologram and the side-band containing the desired phase information. The former set of problems are conventionally addressed by acquiring a reference hologram in a field-free vacuum and the latter by limiting the spatial resolution of the phase reconstruction. Within WP4, we have developed ways to improve the accuracy and precision of the phase reconstruction through better calibration methods and introducing automated procedures.

Automated collection of reference holograms

Reference holograms are acquired with a limited number of electrons. The phase reconstructed from the hologram is therefore noisy, simply from counting statistics. Whilst subtracting the reference phase from the phase acquired from the region of interest (which we will call the specimen hologram) will reduce the systematic sources of phase error detailed above, the random noise will increase. Indeed, the acquisition times for the reference and specimen hologram are usually similar, leading to a doubling of the variance of the random phase fluctuations (and a therefore a 40% increase in the standard deviations). It would therefore be desirable to increase the acquisition time of the reference hologram. Unfortunately, drift and microscope instabilities have previously limited this goal.

We have investigated, whether a dynamic automation of the microscope can allow much longer exposure times for acquiring reference holograms [1]. The automation routines developed by TOU for the Hitachi-I2TEM microscope (Hitachi HF3300-C) were adapted and reproduced on the Holo-TEM (FEI Titan) at JUL within WP11. Series of reference holograms were then acquired over very long exposure times on both machines (see Figure 1).

Automated acquisition of reference hologram series on Hitachi-I2TEM (TOU) with Gatan-OneView CCD camera

Phase error from electron dose Constant phase error

$$\sigma^2(\phi) = \frac{\sigma_e^2}{N_e} + \sigma_\infty^2$$

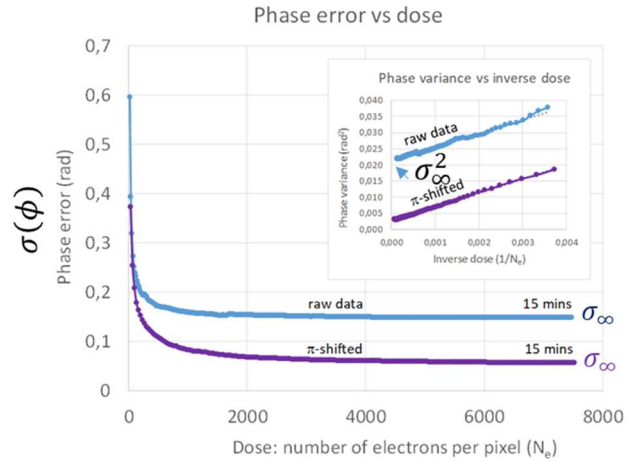


Figure 1. Automated reference hologram acquisition: phase noise as a function of acquisition time, expressed in electron dose, for conventional holograms (blue) and pi-shifted holograms (purple). In both cases, the phase noise decreases initially until a floor is reached. The progression can be modelled (see Equation) as a combination of random noise from counting statistics and a constant phase error.

Holograms were acquired continuously up to 15 minutes, with outputs every 4s to monitor the progress. The phase was reconstructed from each hologram and the standard deviation measured. The results were then plotted as a function of the electron dose (blue curve in Figure 1). Increasing the exposure time from 4s, a typical value for a non-automated microscope, to 1 minute produces a dramatic reduction in the reference hologram phase noise by a factor of more than 3. The use of automated routines for reference hologram acquisition is therefore of considerable benefit.

However, after the initial steep decline in the noise, a plateau is reached with little improvement even after 15 minutes of exposure time. We can model this behaviour by assuming that in addition to the noise from the counting statistics, an uncorrelated but constant phase variation exists, which adds to the noise. The plot of phase variance against the inverse dose (see insert on Figure 1) confirms the validity of this description. It should be noted that the visibility of the hologram is not degraded in any way over the whole exposure time, so the reason needs to be found elsewhere.

[Automated routines for eliminating centre-bands](#)

The second source of error that we have aimed to eliminate is linked to the so-called centre-band of the electron hologram. It was also our initial candidate for the mysterious constant phase noise. Routines have previously been published to remove the centre-band, notably a method, which we call the pi-shift method [2]. Two holograms are acquired with a phase difference of exactly pi, and by subtraction of the two, a “pi-shifted” hologram is obtained, which has the centre-band eliminated. Shifting the phase of a hologram by exactly pi changes the sign of the side-band but not the centre-band. Whilst mathematically elegant, the experimental difficulty has lain in obtaining two identical holograms shifted by exactly pi radians. This means either allowing for luck – letting the hologram drift – or by delicate adjustment of the tilt of the incident beam by adjustment of the instrument

controls by hand. A happy side-effect of dynamic automation makes this method completely routine and reproducible.

Dynamic automation relies on controlling the position of the hologram fringes to high precision and in real time [1]. It was therefore relatively straight-forward to develop a routine to automatically acquire the two holograms shifted by π radians, and create the π -shifted hologram. An example can be seen in Figure 2 acquired on the Hitachi-I2TEM microscope in TOU. On the left is the conventional hologram, albeit acquired over 15 minutes, and on the right, the equivalent π -shifted hologram. The improvement is striking. The source of the improvement can perhaps be better understood in the power spectra of the corresponding holograms. The removal of the centre-band in the π -shifted hologram reduces the background noise (the two power spectra are shown on exactly the same intensity scale). The additional benefit is that a larger mask can be used for the phase reconstruction, resulting in a higher spatial resolution in the phase information.

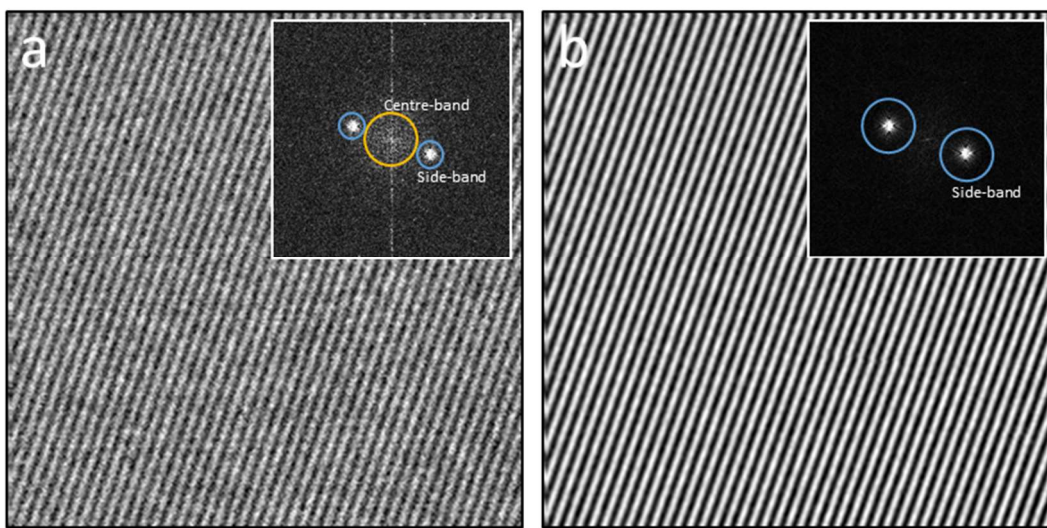
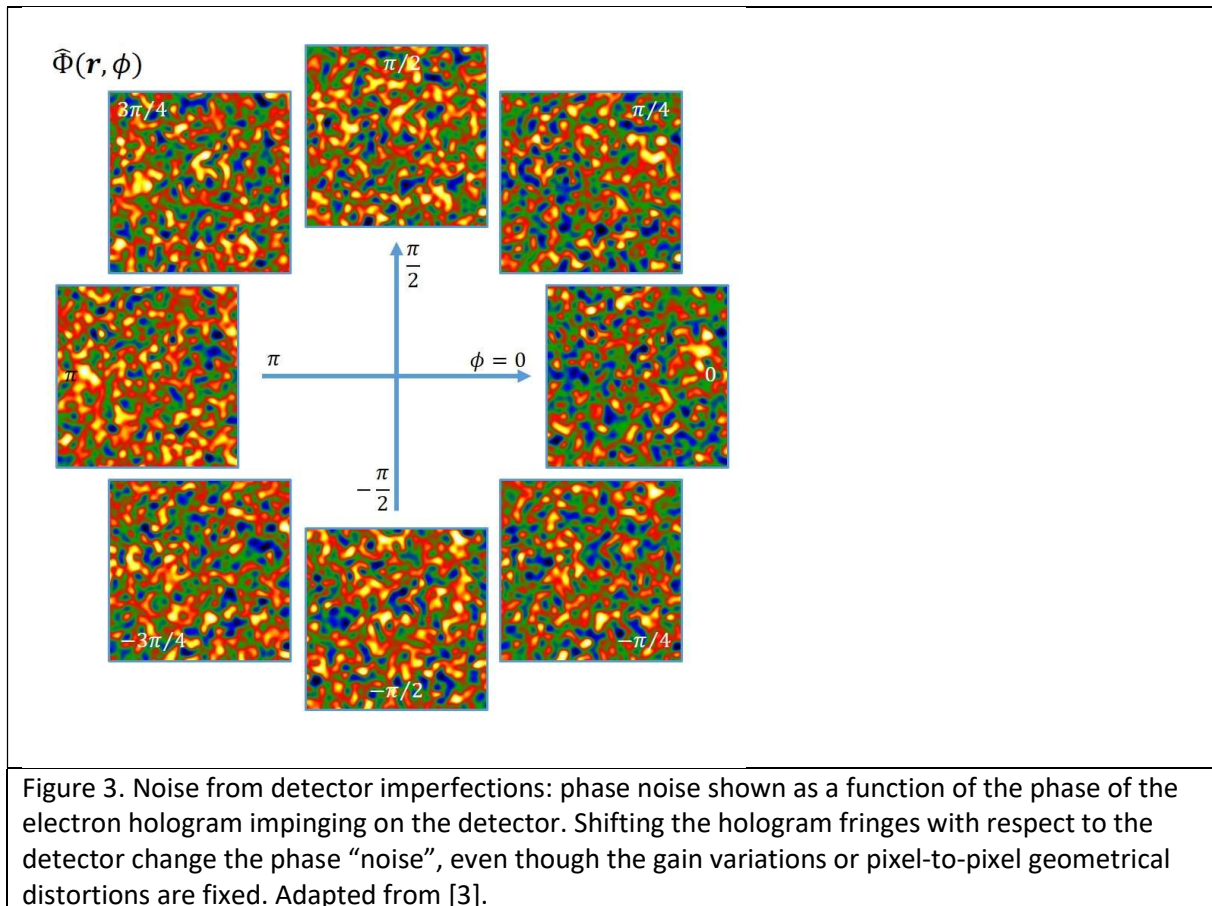


Figure 2. Automated routine to eliminate centre-band: (a) conventional hologram acquired over 15 minutes using dynamic automation, power spectrum (inset) shows centre-band (orange) and side-bands (blue); (b) corresponding π -shifted hologram, power spectrum (inset). The total electron dose is the same for both. Absence of centre-band reduces noise and allows higher spatial resolution for the phase reconstruction.

To test the new procedure, we repeated the series of reference holograms shown previously and under identical experimental conditions. The results are plotted on Figure 1. The π -shifted holograms reduce the noise by a factor of about 3 with respect to the conventional holograms, but still attain a plateau beyond which the noise no longer decreases. These experiments were repeated on the Holo-Titan at JUL with similar results.

[New calibration procedure using multiple reference holograms](#)

These results led us to investigate the possibility that detector imperfections were the cause of the phase noise limit. We considered two causes: imperfect gain normalisation and pixel-to-pixel geometrical distortions. A theoretical study was carried out and the results tested on simulated holograms, the major findings were published in an ESTEEM3 paper [3]. In short, theory and simulation show that the presence of either of these two imperfections introduces noise in the hologram that depends on the phase of the hologram fringes (see Figure 3).



This means the use of a reference hologram may even be counterproductive. Only if the position of the specimen hologram fringes coincides exactly with the reference hologram, this phase noise will be eliminated, and this cannot be achieved across the whole field of view except in the trivial case of two holograms taken in field-free vacuum.

Diffraction calibration with a sample-space deflector

The projection system of a TEM contains a large number of degree of freedom. Thus, it is no surprise that, despite the usage of standardized alignment procedures by the manufacturers, the magnification or the equivalent camera lengths can have relevant differences, even between identical instruments. This causes the need to perform relative calibrations using reference samples on each microscope, which is however problematic in itself, as the microscope can image scales ranging from tens of microns to tens of picometers, thus spanning at least 6 orders of magnitude. Therefore, it is impossible to find reference samples offering well-characterised reference structures across such a wide range. Furthermore, these calibrations can be influenced by a number of factors and they need to be re-acquired with a certain regularity, though this is often not done.

A standardless procedure capable of performing calibration from first principles would alleviate many of these limitations, and its feasibility has been investigated. By subjecting the electron beam to a transverse field, we can induce a deflection, which is strictly proportional to the field strength. The simplest realisation of such a setup would be a parallel plate capacitor, where the electrical field is uniform along the direction of travel of the electron, allowing to straightforwardly calculating the deflection. An alternative approach would be to use a transverse magnetic field, generated by a couple of magnetic coils, but the strong fields and delicate conditions in the sample plane make it

unfeasible to use magnetic materials for the coils' core, making it hard to achieve high enough field strength. Such magnetic cores would also give us a nonlinear relation between coil current and deflection, a feature we really avoid in a calibration tool. Even in the case of so-called air coils without ferromagnetic core material, we would still have the magnetisation of the nearby pole pieces to take into account, resulting again in unwanted non-linearities and hysteresis effects.

We therefore opted for electrostatic deflection and manufactured one such prototype by hand and introduced it in the microscope with a DENS Solutions Wildfire electrical contact holder.

We then expect the application of a potential to lead to a proportional deflection. The tests (Figure 4) indeed show this deflection to be linear and reproducible, and to depend very weakly on the z-position of the stage, even across the full range of motion of the stage, proving the robustness of the approach and how it's robust against operator error.

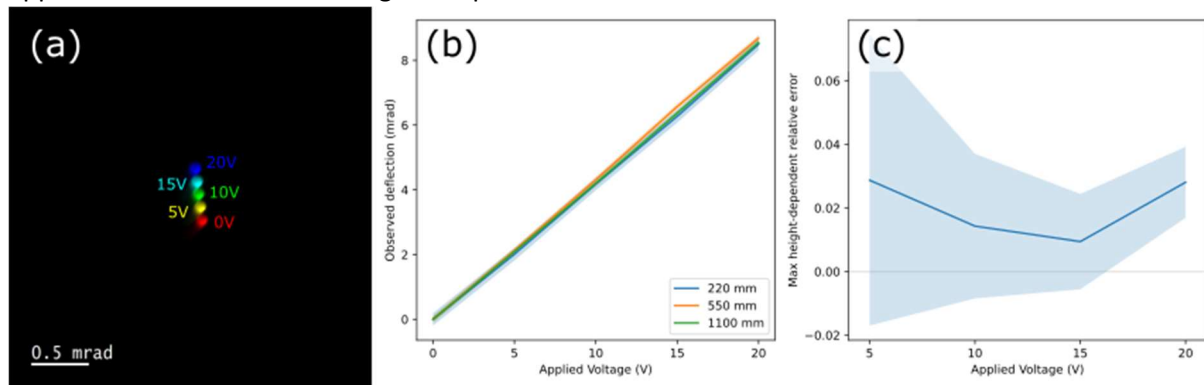


Figure 4. Deflection induced by a capacitor. (a) The diffraction spot is shifted by the application of a known potential. The spot is intentionally made wider in order to minimise streaking on the CCD detector. (b) The deflection at different camera lengths. The difference is below the uncertainty of 1 pixel (shaded areas). (c) The experiment has been repeated at different heights across the stage's z-range (-300 to 300 μm) and the highest (relative) deviation from the original value is indicate. The shaded area indicates 1-pixel uncertainty. The deviation appears weakly sensitive to even widely exaggerated positioning errors.

Combining this device with a programmable scanning unit, such as the developed at CNRS-LPS laboratory (Laboratoire de Physique des Solides, Orsay, France), would allow to quickly switch between voltages obtaining a lattice of points, allowing a more immediate calibration and better management of the beam intensity.

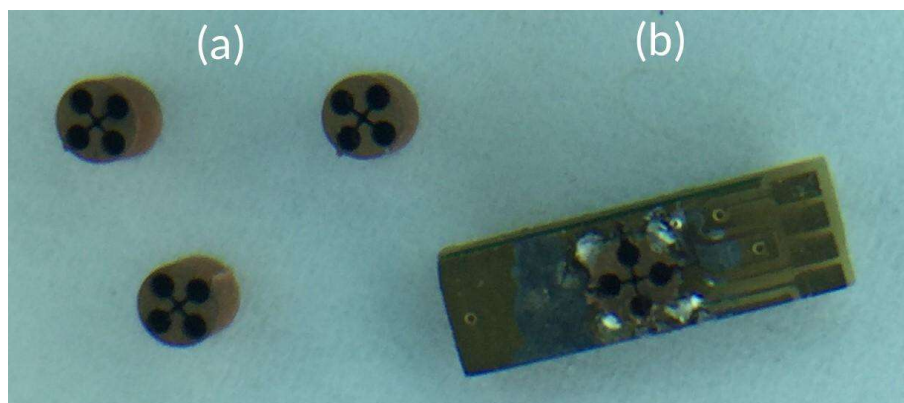


Figure 5. (a) Prototype quadrupoles produced with wire EDM cutting in copper (2 mm diameter). By setting two adjacent electrodes to the same potential (and the other two electrodes to the opposite potential), a uniform electrical field is created in the central gap. This allows two-dimensional deflections in either direction. (b) Quadrupole mounted on a carrier PCB compatible with the Dens Solutions Wildfire holder

The next step is the development of a new design based on an electric quadrupole, capable of deflecting the beam in two perpendicular directions. In order to reach a reproduceable small gap, we fabricated a quadrupole shape with 100 um gaps with electrical discharge micromanufacturing (EDM). This method would potentially allow to reproduce a calibration device that can be manufactured at an acceptable cost and could offer interesting product opportunities for the SME's involved in ESTEEM3. We mount the quadrupole on a custom made PCB that fits into a Dens Wildfire sample holder, offering a versatile solution compatible with a range of different vendor TEM instruments.

When combined with a programmable scanning unit, this will allow to project a two-dimensional lattice of points, yielding a straightforward calibration of camera length as well as non-linear distortions in the projection system. If the control voltage can be made with a 16-bit dac, a dynamic range of almost 5 orders of magnitude can be made. The design of this improved prototype has been completed, the fabrication is underway and several milestones have already been reached (Figure 5).

Improved corrector alignment

Nowadays, most state-of-the-art electron microscopes include aberration correctors. The corrector fine-tuning for daily operation, however, still requires considerable knowledge and experience to achieve optimum optical performance. CEOS has recently automated the alignment procedures for correctors in TEM and STEM for daily operation. The auto-alignment routines automatically select suitable measurement conditions and 'decide' about further correction steps not only depending on the measured residual aberrations, but also take into account the measurements' confidence. The special emphasis on error recognition enables a robust automatic tuning procedure, which minimizes the amount of time, which is required for the daily corrector tuning. Figure 6(a-c) shows the auto-alignment procedure for the CEOS image corrector (CETCOR).

There is a growing number of special (S)TEM applications, which do not require the aberration corrector to perfectly correct all aberrations, but to tailor the electron optical conditions in a very well-defined way (phase shaping). For this purpose, it is very important to give feedback to the user what is experimentally feasible under existing conditions and to compare with the presently measured state. For this purpose, recently a probe simulation has been built into the STEM corrector software in order to visualize the currently measured probe shape and to relate it to the theoretical limits of the present microscope setup, see Figure 6(d). Subsequent changes of the corrector's calibrated alignment tools are immediately taken into account in the probe calculation to provide a reliable prediction about the probe shape. Correspondingly, in the TEM corrector software a simulation of the phase contrast transfer function is provided.

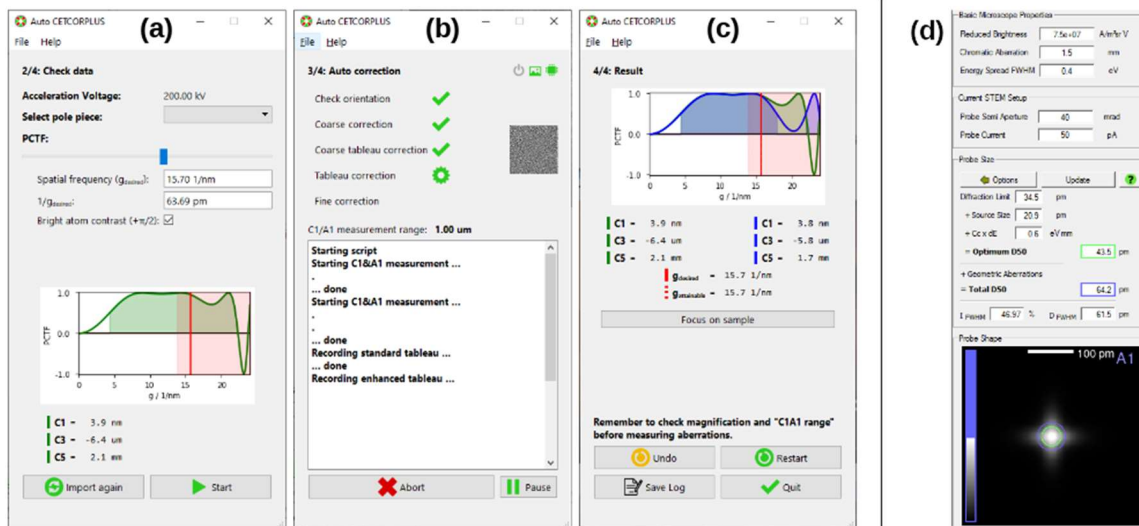


Figure 6. (a-c) Corrector auto-tune for CETCOR: (a) after initial selection of desired parameters, the tuning towards the desired state is done automatically (b). The procedure's result (c) is finally presented to the user to proceed with the experimental session. An equivalent workflow is available for CEOS' probe correctors. - The probe simulation (d) provides immediate feedback to the user about the setup's instrumental limits and the present optical performance.

Future development

The plan for future development of the fringe-based calibration is to test the new theory experimentally and to develop a method involving multiple reference holograms to solve the problem of correcting specimen holograms across the whole field of view. Initial results are highly encouraging. Beyond electron holography, the implications for high-resolution TEM and detector calibration will be explored.

For the first-principle-calibration procedure using electromagnetic deflectors, the new quadrupolar deflector needs to be finalised and put into operation. Particular attention is being paid to the possibility of mass producing the final design so that it can be widely deployed in a cost-effective way, at a sub-200€ price point, and to this end only common and scalable fabrication methods have been used. The quadupoles have been fabricated in copper by an electrical discharge machining, and the carrier chips using standard PCB fabrication, but a reliable procedure for assembling the final device is still being investigated. The feasibility of a magnetic alternative, based on air-core coils, will also be explored.

CEOS continuously tries to improve the corrector software to relieve the microscopist in terms of alignment efforts and to improve on feedback about the optical state and its consequences for the desired experiment.

Software

[A]

References

- [1] C. Gatel, J. Dupuy, F. Houdellier, M.J. Hýtch, Appl. Phys. Lett. 113, 133102 (2018). *Unlimited acquisition time in electron holography by automated feedback control of transmission electron microscope*. [10.1063/1.5050906](https://doi.org/10.1063/1.5050906)
- [2] V. V. Volkov, M. G. Han, Y. Zhu, Ultramicroscopy 134, 175–184 (2013). *Double resolution electron holography with simple Fourier transform of fringe-shifted holograms*. [10.1016/j.ultramic.2013.06.018](https://doi.org/10.1016/j.ultramic.2013.06.018)
- [3] M.J. Hýtch and C. Gatel, Microscopy 70, 47–58 (2021). *Phase detection limits in off-axis electron holography from pixelated detectors: gain variations, geometric distortion and failure of reference-hologram correction*. [10.1093/jmicro/dfaa044](https://doi.org/10.1093/jmicro/dfaa044). **ESTEEM3**.